ISSN 0967-0912, Steel in Translation, 2017, Vol. 47, No. 6, pp. 369–373. © Allerton Press, Inc., 2017.
Original Russian Text © Yu.F. Ivanov, E.G. Belov, V.E. Gromov, S.V. Konovalov, D.A. Kosinov, 2017, published in Izvestiya Vysshikh Uchebnykh Zavedenii, Chernaya Metallurgiya, 2017, No. 6, pp. 457–462.

Structure and Properties of I-Beams after Accelerated Water Cooling

Yu. F. Ivanov[a, b, *], **E. G. Belov**[c, **], **V. E. Gromov**[d, ***], **S. V. Konovalov**[e, ****], **and D. A. Kosinov**[d, *****]

[a]Institute of High-Current Electronics, Siberian Branch, Russian Academy of Sciences, Tomsk
[b]Tomsk Polytechnic University, Tomsk
[c]AO EVRAZ Zapadno-Sibirskii Metallurgicheskii Kombinat (AO EVRAZ ZSMK), Novokuznetsk
[d]Siberian State Industrial University, Novokuznetsk
[e]Korolev Samara National Research University, Samara
*e-mail: yufi@mail.ru
**e-mail: belov_eg@zsmk.ru
***e-mail: gromov@physics.sibsiu.ru
****e-mail: kosinov.dima@rambler.ru
*****e-mail: ksv@ssau.ru

Received May 5, 2017

Abstract—The structure and properties of the surface of DP155 I-beams made of 09G2S low-carbon steel are determined on the basis of materials physics, before and after thermomechanical strengthening—that is, accelerated water cooling. Such I-beams are used in monorail tracks. Highly defective structure in the surface layer is created by accelerated cooling of the beam in the line of the 450 bar mill at AO EVRAZ Zapadno-Sibirskii Metallurgicheskii Kombinat, in the following conditions: rolling speed 6 m/s; water pressure in the crosspiece-cooling section 0.22–0.28 MPa; temperature before cooling about 800°C. As a result, the hardness, wear resistance, and scalar dislocation density are higher than in the steel without strengthening. Without thermal strengthening, the microhardness of the samples is 2.70 ± 0.33 GPa, while the Young's modulus is 269.2 ± 27.1 GPa. Thermomechanical strengthening increases its microhardness to 3.30 ± 0.29 GPa, and decreases the Young's modulus to 228.2 ± 25.7 GPa. In addition, the microhardness range is increased from 2.20–3.80 GPa to 2.64–4.60 GPa, while the Young's modulus range is reduced from 208.0–403.0 GPa to 184.1–278.2 GPa on thermomechanical strengthening. It is found that thermomechanical strengthening increases the wear resistance of the steel's surface layer by a factor of ~1.36 (decrease in wear rate from 5.3×10^{-5} to 2.9×10^{-5} mm^2/N m) and increases the frictional coefficient by a factor of 1.36 (from 0.36 to 0.49). Without thermal strengthening, the structure observed is dislocational chaos; the scalar density of the dislocations is $(0.9–1.0) \times 10^{10}$ cm^{-2}. High-temperature rolling and subsequent accelerated cooling of the samples produces dislocational substructure of band type in the ferrite grains and of reticular type in the martensite grains: the mean scalar density of the dislocations in the surface layer is 4.5×10^{10} cm^{-2}. Possible explanations for such behavior are discussed.

Keywords: thermomechanical strengthening, I-beams, structure, dislocational substructure, tribological properties

DOI: 10.3103/S0967091217060055

In materials physics, it is important to understand the evolution of structural and phase states and defect substructure in steels, in order to improve their performance [1–11]. In the last decade, thermomechanical strengthening—accelerated water cooling—has been widely adopted in rolling technology. To create the required strength and plasticity of steel, we need to understand the physical changes in such strengthening, under the action of complex deformation and heating. In studying thermomechanical strengthening, we must establish the relations between the mechanical properties of the product and the evolution of the structural and phase states and defect substructure for each rolled product if we are to ensure optimal treatment and specify the required properties.

Monorail tracks are produced from thermomechanically strengthened DP155 I-beams, which ensure high load capacity and reliability under intense mechanical forces in dusty air. The structural and phase states and defect substructure for such I-beams were studied in [12–15]. That provides the physical basis for specifying the properties over the length and

Table 1. Chemical composition of 09G2S steel

Steel	Content, %							
	C	Si	Mn	S	P	N	V	Al
09G2S	0.087	0.62	1.36	0.012	0.019	0.0071	0.004	0.011
GOST 19281 specifications	0.07–0.12	0.50–0.80	1.30–1.70	≤0.035	≤0.035	0.008	–	≤0.05

cross section such that buckling is prevented. The lateral surface of the crosspiece is under the greatest load. Consequently, it is of scientific and practical interest to study the structure and tribological properties of the crosspiece. That is the aim of the present work.

We investigate DP155 I-beams (class 345) produced with accelerated cooling in the line of the 450 bar mill at AO EVRAZ Zapadno-Sibirskii Metallurgicheskii Kombinat (AO EVRAZ ZSMK).

Experimental batches of I-beams are produced from 150 × 200 mm continuous-cast 09G2S steel billet, whose chemical composition corresponds to State Standard GOST 19281, as we see in the Table 1.

The thermomechanical strengthening (accelerated cooling) of the rolled steel ensures mechanical properties of class 345. The cooling configuration and the temperatures and cooling rates employed in thermomechanical strengthening may be found in [12–15]. For comparison, we also investigate the structure and properties of 09G2S steel beams produced without thermomechanical strengthening, with a final rolling temperature of ~~100~~°C.

The phase composition and defect substructure of the steel are investigated by the diffractional electron microscopy of thin foil [16–20]. The working magnification in the electron microscope is 8000–80000. The final magnification is established by means of photographic printing or computer graphics. In Fig. 1, we show the preparation of the sample from the I-beam in the production of thin foil. A plate of thickness about 0.3 mm adjacent to the I-beam surface is cut from the sample by electrospark machining. The plate is mechanically thinned to 100–150 μm and polished on one side in 450 ml H_3PO_4 electrolyte and 50 g chromium anhydride, at a voltage of 20–27 V and current density of 2–3 A/cm^2, so as to obtain a thickness of about 200 nm suitable for electron-microscope study.

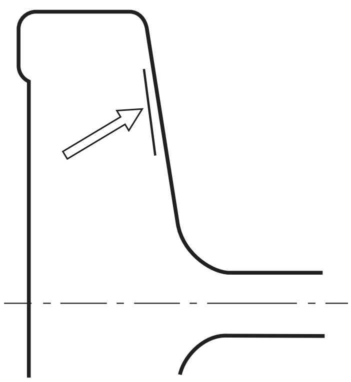

Fig. 1. Preparing a sample of the I-beam in producing foil for analysis by diffractional transmission electron microscopy. The arrow indicates the position of the plate used in foil production.

The nanohardness and Young's modulus of the surface layer are determined on a Shimadzu DUH-211S dynamic system, with a load of 50 mN on the nanoindenter. The wear resistance of the steel is analyzed on an S/N 07-142 high temperature tribometer (CSEM, Switzerland) and a Tribotechnic (France) instrument, with determination of the frictional coefficient and wear rate. The counterbody is a VK6 hard-alloy ball (diameter 3 mm). The measurements are made with rotation of the sample at a motionless counterbody. The linear rotation speed is 2.5 cm/s. The normal load on the counterbody is 5 N; the final number of sample rotations is 5000. At the end of the frictional process, the profile of the frictional groove in the sample surface is measured by means of a Micro Measure 3D station (STIL, France) and a Tribotechnic (France) instrument, with numerical determination of the depth and cross-sectional area of the frictional groove. The wear resistance is calculated as the inverse of the wear rate V (mm^3/N m), which takes the form

$$V = \frac{2\pi RA}{FL},$$

Here R is the track radius, mm; A is the cross-sectional area of the frictional groove, mm^2; F is the applied load, N; and L is the dilation of the counterbody (ball), m.

In Fig. 2, we show the structure of 09G2S steel without thermomechanical strengthening, according to diffractional transmission electron microscopy. Morphological and microdiffractional analysis shows that

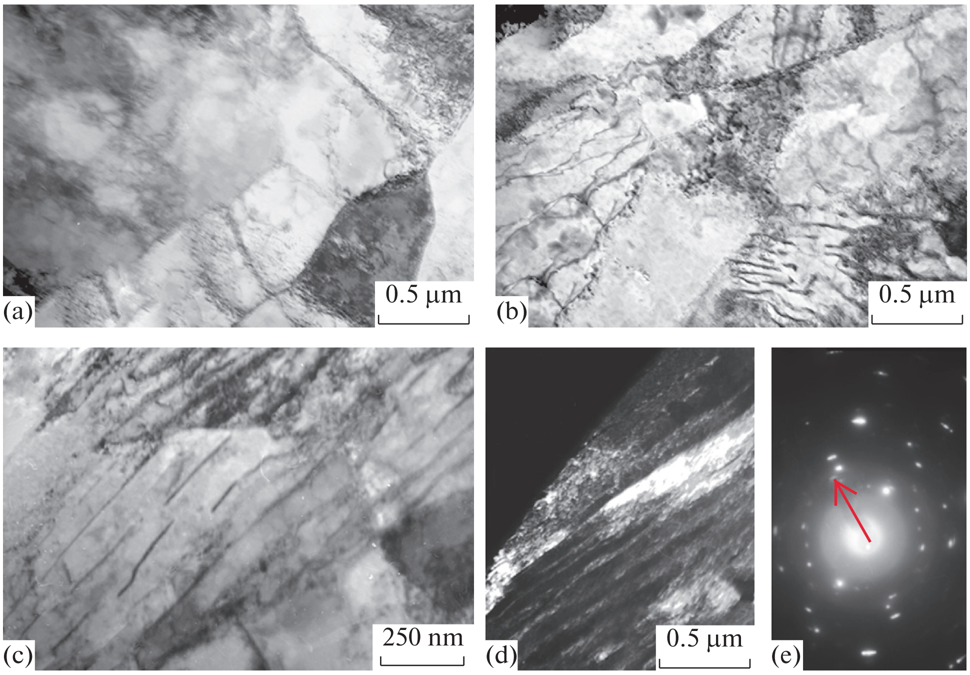

Fig. 2. Electron-microscope images of the structure of 09G2S steel without thermomechanical strengthening: (a–c) light-field image; (d) dark-field image obtained in the close reflexes [320] Fe_3C and [002] α Fe; (e) electron-diffraction pattern. The arrow indicates the reflex in which the dark field is produced.

the ferrite grain is the basic structural component of the steel (Figs. 2a and 2b). The content of pearlite grains of plate type is significantly lower (Figs. 2c and 2d). Dislocational substructure is seen within the ferrite grains and the ferrite component of the pearlite grains. The distribution of the dislocations is predominantly chaotic (dislocational chaos [21]). The scalar dislocation density, determined by the secant method, is (0.9–1.0) × 10^{10} cm^{-2} [16–20].

After high-temperature rolling and subsequent accelerated cooling, the surface layer of the I-beam is characterized by quenched structure: the ferrite grains are accompanied by grains containing martensite crystals of packet morphology. No pearlite grains are seen in the surface layer of the I-beam. At a distance of 4 mm or more, the steel structure consists of ferrite and pearlite grains. No martensitic structure is seen.

As we see in Fig. 3, the defect substructure of the ferrite grains in the surface layer of the steel consists mainly of deformation bands (band substructure; 75% of the grain volume). In smaller quantities, we note substructure in the form of dislocational chaos (20% of the grain volume) and subgrains (5% of the grain volume). In the martensite crystals, we see reticular dislocational substructure. The mean scalar dislocation density over all types of substructure in the surface layer of the thermostrengthened I-beam is 4.5 × 10^{10} cm^{-2}.

Thus, thermomechanical strengthening of 09G2S steel leads to the formation of morphologically complex defect substructure in the surface layer of the I–beam, with relatively high scalar dislocation density. Obviously, such transformation of the defect substructure must be accompanied by improved performance of the steel.

The nanohardness and Young's modulus of 09G2S steel before/after thermomechanical strengthening are as follows:

Characteristic	Value			
	mean	error	minimum	maximum
Hardness, GPa	$\frac{2.70}{3.30}$	$\frac{0.33}{0.29}$	$\frac{2.20}{2.64}$	$\frac{3.80}{4.60}$
Young's modulus, GPa	$\frac{269.6}{228.2}$	$\frac{27.1}{25.7}$	$\frac{208.0}{184.1}$	$\frac{403.0}{278.2}$

It is evident that the thermomechanical strengthening is accompanied by increase in hardness of the surface layer by a factor of about 1.22, with about 1.18-fold decrease in the Young's modulus. The strengthening of the steel significantly changes its tribological characteristics: the wear resistance of the surface layer and the frictional coefficient are increased by factors of about 1.83 and 1.36, respectively. The wear rate of the steel is 5.3 × 10^{-5} before thermomechanical strengthening and 2.9 × 10^{-5} m^3/N m after strengthening; the corresponding values of its frictional coefficient are 0.36 and 0.49.

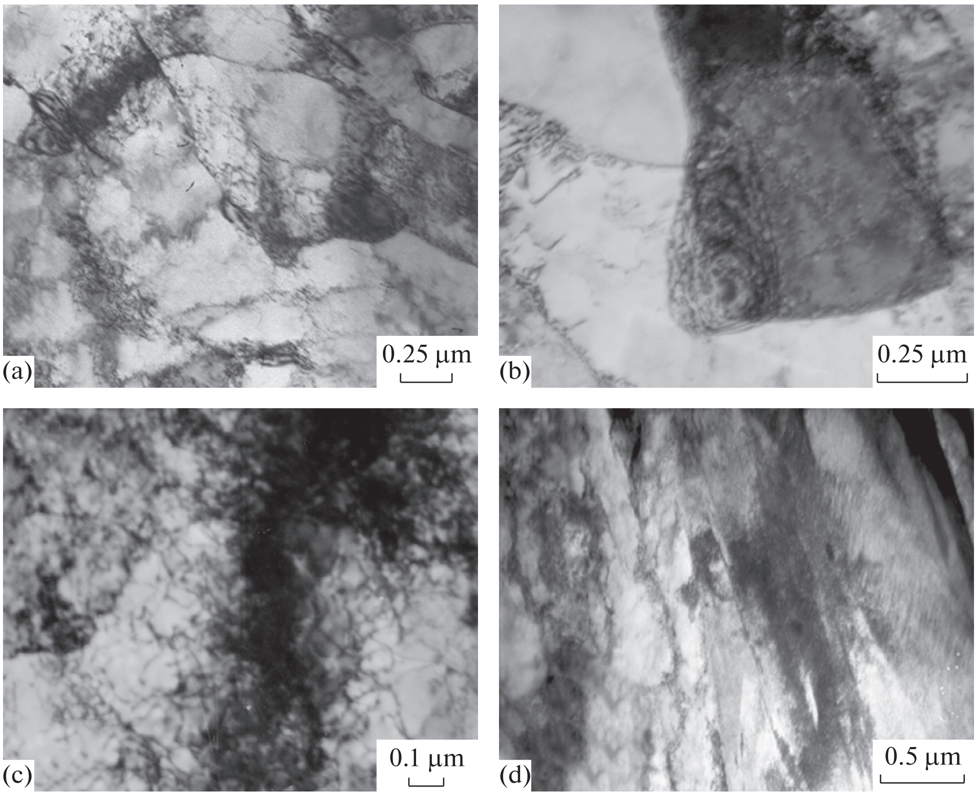

Fig. 3. Electron-microscope images of the defect substructure formed in ferrite grains of the surface layer of the I-beam on thermomechanical strengthening: (a) band substructure; (b, c) subgrain and reticular substructure; (d) martensite crystals.

CONCLUSIONS

The defect substructure of 09G2S steel before and after thermomechanical strengthening is studied by diffractional transmission electron microscopy.

Accelerated cooling of the steel in the line of the 450 bar mill at AO EVRAZ Zapadno-Sibirskii Metallurgicheskii Kombinat produces a surface layer of highly defective structure, with increased hardness and wear resistance. The Young's modulus and frictional coefficient are lower by a factor of 1.2–1.3 after thermomechanical strengthening.

ACKNOWLEDGMENTS

Financial support was provided by the Russian Foundation for Basic Research (grants 16-48-420530r_a and 16-32-60048mol_a_dk; project 3.1283.2017/PCh).

REFERENCES

1. Rethinam, A., Shivakumar, V.D., Harish, L., Abhishek, M.B., Ramana, G.V., Madhusudana, R., Sah, R., and Manjini, S., Grain refinement of C–Mn steel through thermo-mechanical processing, *J. Eng., Des. Technol.*, 2015, vol. 13, no 2, pp. 282–297.
2. He, L., Zhang, H., and Cui, J., Effects of thermomechanical treatment on the mechanical properties and microstructures of 6013 alloy, *J. Wuhan Univ. Technol., Mater. Sci. Ed.*, 2009, vol. 24, no. 2, pp. 198–201.
3. Nemecek, S., Novy, Z., and Stanková, H., Optimization of heat treatment of TRIP steels, *Metall. Ital.*, 2006, vol. 98, no 2, pp. 47–51.
4. Bakkaloglu, A., Effect of thermomechanical treatment on the microstructure and mechanical properties of HSLA steels, *Modell., Meas. Control, C*, 1994, vol. 44, nos. 3–4, pp. 39–50.
5. Kaputkina, L.M., Bernshtein, M.L., and Zaimovskii, V.A., *Termomekhanicheskaya obrabotka stali (Thermomechanical Treatment of Steel)*, Moscow: Metallurgiya, 1983.
6. Chen, X., Huang, Y., and Lei, Y., Microstructure and properties of 700 MPa grade HSLA steel during high temperature deformation, *J. Alloys Compd.*, 2015, vol. 631, pp. 225–231.
7. Chen, X. and Huang, Y., Hot deformation behavior of HSLA steel Q690 and phase transformation during compression, *J. Alloys Compd.*, 2015, vol. 619, pp. 564–571.
8. Tushinskii L.I. *Teoriya i tekhnologiya uprochneniya metallicheskikh splavov* (Theory and technology of metal alloys hardening), Novosibirsk: Nauka, 1990.
9. Starodubov, K.F., Uzlov, I.G., Savenkov, V.Ya., Polyakov, S.N., and Kalmykov, V.V., *Termicheskoe uprochnenie prokata* (Thermal Hardening of Rolled Products), Moscow: Metallurgiya, 1970.

10. Bykhin, B.B., Kanaev, A.T., Kapushchak, A.F., and Kanaev, A.A., Improvement of the thermal strengthening regimes of reinforcing steel bars, *Stal'*, 1998, no. 12, pp. 46–48.

11. Uzlov, I.G., Thermomechanical hardening of rolled metal is an effective way of energy saving and improvement of metal products quality, *Metall. Gornorudn. Prom-st'*, 1999, no. 5, pp. 61–63.

12. Kosterev, V.B., Belov, E.G., Efimov, O.Yu., Yur'ev, A.B., Chinokalov, V.Ya., Ivanov, Yu.F., Konovalov, S.V., and Gromov, V.E., Formation of fine structure and mechanical properties during accelerated cooling of beam profile, *Vestn. Tambovsk. Univ., Ser.: Estestv. Tekh. Nauki*, 2010, vol. 15, no. 3, pp. 825–826.

13. Kosterev, V.B., Gromov, V.E., Ivanov, Yu.F., Efimov, O.Yu., and Yur'ev, A.B., Formation of structural-phase states of the surface of thermal hardening, *Deform. Razrushenie Mater.*, 2010, no. 10, pp. 43–46.

14. Kosterev, V.B., Efimov, O.Yu., Ivanov, Yu.F., Belov, E.G., and Gromov, V.E., Formation of gradient structure-phase states in thermomechanical hardening, *Steel Transl.*, 2011, vol. 41, no. 4, pp. 283–286.

15. Kosterev, V.B., Ivanov, Y.F., Gromov, V.E., Efimov, O.Y., and Konovalov, S.V., Formation of structure-phase states and dislocation substructures during thermomechanical hardening of Fe–0.09C–2Mn–1Si steel, *Russ. Phys. J.*, 2012, vol. 54, no. 9, pp. 1034–1045.

16. Hirsch, P.B., Howie, A., Nicholson, R.B., Pashley, D.W., and Whelan, M.J., *Electron Microscopy of Thin Crystals*, Melbourne: Krieger, 1977.

17. Brandon, D. and Kaplan, W.D., *Microstructural Characterization of Materials*, New York: Wiley, 2008.

18. Zou, X., Hovmöller, S., and Oleynikov, P., *Electron Crystallography: Electron Microscopy and Electron Diffraction*, Oxford: Oxford Univ. Press, 2012.

19. Williams, D.B. and Carter, C.B., *Transmission Electron Microscopy. A Textbook for Materials Science*, New York: Springer-Verlag, 2009.

20. Egerton, R.F., *Physical Principles of Electron Microscopy. An Introduction to TEM, SEM, and AEM*, New York: Springer-Verlag, 2016.

21. Koneva, N.A. and Kozlov, E.V., Nature of substructural hardening, *Sov. Phys. J.*, 1982, vol. 25, no. 8, pp. 681–691.

Translated by Bernard Gilbert

SPELL: 1. ok